A gain-of-function mutation in the CLCN2 chloride channel gene causes primary aldosteronism

Fabio L Fernandes-Rosa, Georgios Daniil, Ian J Orozco, Corinna Göppner, Rami El Zein, Vandana Jain, Sheerazed Boulkroun, Xavier Jeunemaître, Laurence Amar, Hervé Lefebvre, et al.

A gain-of-function mutation in the *CLCN2* chloride channel gene causes primary aldosteronism

Fabio L Fernandes-Rosa[1,2,3*#], Georgios Daniil[1,2*], Ian J Orozco[4,5*], Corinna Göppner[4,5$], Rami El Zein[1,2$], Vandana Jain[6^], Sheerazed Boulkroun[1,2^], Xavier Jeunemaitre[1,2,3], Laurence Amar[1,2,7], Hervé Lefebvre[8,9,10], Thomas Schwarzmayr[11], Tim M Strom[11,12], Thomas J Jentsch[4,5#], Maria-Christina Zennaro[1,2,3#]

[1]INSERM, UMRS_970, Paris Cardiovascular Research Center, Paris, France
[2]Université Paris Descartes, Sorbonne Paris Cité, Paris, France
[3]Assistance Publique-Hôpitaux de Paris, Hôpital Européen Georges Pompidou, Service de Génétique, Paris, France
[4]Leibniz-Forschungsinstitut für Molekulare Pharmakologie (FMP), Berlin, Germany
[5]Max-Delbrück-Centrum für Molekulare Medizin (MDC), Berlin, Germany
[6]Division of Pediatric Endocrinology, Department of Pediatrics, All India Institute of Medical Sciences, New Delhi, India
[7]Assistance Publique-Hôpitaux de Paris, Hôpital Européen Georges Pompidou, Unité Hypertension artérielle, Paris, France
[8]Normandie Univ, UNIROUEN, Rouen, France
[9]INSERM, DC2N, Rouen, France
[10]Department of Endocrinology, Diabetes and Metabolic Diseases, University Hospital of Rouen, Rouen, France
[11]Institute of Human Genetics, Helmholtz Zentrum München, Neuherberg, Germany
[12]Institute of Human Genetics, Technische Universität München, Munich, Germany
*,$,^equal contribution
#Corresponding authors

Address correspondence to:
Maria-Christina Zennaro, MD, PhD
INSERM, U970
Paris Cardiovascular Research Center – PARCC
56, rue Leblanc,
75015 Paris – France
Tel : +33 (0)1 53 98 80 42
Fax : + 33 (0)1 53 98 79 52
e-mail : maria-christina.zennaro@inserm.fr

Fabio Fernandes Rosa, MD, PhD
INSERM, U970
Paris Cardiovascular Research Center – PARCC
56, rue Leblanc,
75015 Paris – France
Tel : +33 (0)1 53 98 80 43
Fax : + 33 (0)1 53 98 79 52
e-mail : fabio.fernandes-rosa@inserm.fr

Thomas J. Jentsch, MD, PhD
FMP / MDC
Robert-Rössle-Strasse 10
13125 Berlin – Germany

Tel: +49 30 9406 2961
Fax: +49 30 9406 2960
e-mail: Jentsch@fmp-berlin.de

INTRODUCTORY PARAGRAPH

Primary aldosteronism is the most common and curable form of secondary arterial hypertension. We performed whole exome sequencing in patients with early-onset primary aldosteronism and identifed a *de novo* heterozygous c.71G>A/p.Gly24Asp mutation in the *CLCN2* gene, coding for the voltage-gated ClC-2 chloride channel [1], in a patient diagnosed at age 9 ys. Patch-clamp analysis of glomerulosa cells of mouse adrenal gland slices revealed hyperpolarization-activated Cl^- currents that were abolished in *Clcn2*$^{-/-}$ mice. The p.Gly24Asp mutation, located in a well conserved 'inactivation domain' [2,3], abolished the voltage- and time-dependent gating of ClC-2 and strongly increased Cl^- conductance at resting potentials. Expression of ClC-2_{24Asp} in adrenocortical cells increased expression of aldosterone synthase and aldosterone production.

Our data indicate that *CLCN2* mutations cause primary aldosteronism. They highlight for the first time the important role of chloride in aldosterone biosynthesis and identify ClC-2 as the foremost chloride conductor of resting glomerulosa cells.

MAIN TEXT

Arterial hypertension is a major cardiovascular risk factor [4]. Primary aldosteronism is the most common and curable form of secondary arterial hypertension, with an estimated prevalence of ~10% in referred patients and 4% in primary care[5], and up to 20% of patients with resistant hypertension [6]. Primary aldosteronism results from autonomous aldosterone production in the adrenal cortex [7], caused in most cases by a unilateral aldosterone-producing adenoma or bilateral adrenal hyperplasia (BAH). It is diagnosed on the basis of hypertension associated with increased aldosterone to renin ratio and often hypokalemia [8]. Compared to essential hypertension, increased aldosterone levels in primary aldosteronism are associated with increased cardiovascular risk in particular coronary artery disease, heart failure, renal damage and stroke [9,10].

Gain-of-function mutations in different genes, coding for cation channels (*KCNJ5* [11], *CACNA1D* [12,13], *CACNA1H* [14,15]) and ATPases (*ATP1A1* and *ATP2B3*, [12,16]), regulating intracellular ion homeostasis and plasma membrane potential, have been described in aldosterone producing adenoma and familial forms of primary aldosteronism, but the pathophysiology of many cases is still unknown.

We performed whole exome sequencing on germline DNA from 12 patients with young onset hypertension and hyperaldosteronism diagnosed before age 25 ys. Two index cases were investigated together with their parents and unaffected sibling to search for *de novo* variants. A *de novo* germline *CLCN2* variant c.71G>A (NM_004366; p.Gly24Asp) was identified in subject K1011-1, but not in her asymptomatic parents (K1011-3 and K1011-4) and sibling (K1011-2, Fig. 1a and 1b, Table 1). The variant was absent from more than 120.000 alleles in the Exome Aggregation Consortium (ExAC) and in our in-house database. We did not find additional *CLCN2* variants among the other 11 investigated individuals. *CLCN2* encodes the chloride channel ClC-2. The variant *CLCN2* p.Gly24Asp localizes to its N-terminal cytoplasmic domain (Fig. 1c, d). Gly24 is highly conserved in ClC-2 orthologs of species as distant as zebrafish and *Xenopus* (Fig. 1c).

The patient carrying the *CLCN2* p.Gly24Asp variant is a 9 year old girl, who presented with severe headache and vomiting lasting for 1 year (Table 1). The child was developmentally normal, first born to a non-consanguineous couple. There was history of mild hypertension in maternal grandmother and granduncle. Blood pressure (BP) was 172/100 mm Hg, heart rate was 120/minute. The rest of the examination was normal. Her work-up revealed persistent hypokalemia (serum K^+ ranging from 1.8 to 2.4 meq/L), elevated serum aldosterone (868.1 pg/ml, reference range 12-340 pg/ml) and suppressed plasma renin activity (0.11 ng/ml/hr, reference range 1.9 to 6.0 ng/ml/hr in upright posture), suggestive of primary aldosteronism. Abdominal CT scan showed no adrenal abnormalities. Other parameters including 24 hours urinary vanillylmandelic acid and serum cortisol were normal. Hypertension was initially managed with amlodipin, enalapril and atenolol. Once the diagnosis of primary aldosteronism was made, spironolactone was added, enalapril was stopped and doses of amlodipin and atenolol were reduced. Serum K^+ normalized. A positive glucocorticoid suppression test (aldosterone 949.3 pg/ml at baseline and 56.9 pg/ml after

administration of oral dexamethasone 0.5 mg every 6 hours for 48 hours) suggested the possibility of glucocorticoid remediable aldosteronism (GRA), a rare familial form of hyperaldosteronism [17]. However, genetic analysis for a chimeric *CYP11B1*/*CYP11B2* gene was negative. The child's hypertension has been well controlled over the last 18 months with prednisolone 5mg/m^2/day, spironolactone and amlodipin. On treatment, her serum aldosterone and plasma renin are 421 pg/ml (reference range 25 to 392) and 8.22 μU/mL (4.4 to 46.1). After exclusion of GRA by genetic testing, prednisolone treatment was stopped.

Cl^- conductances can regulate the excitability of neuronal, muscle, and endocrine cells [18-21] . In zona glomerulosa cells, ACTH-activated Cl^- currents have been described [22], but their outward rectification sets them apart from hyperpolarization-activated ClC-2 currents. ClC-2 is expressed in almost all tissues [1] and may have roles in ion homeostasis and transepithelial transport [23]. *Clcn2*$^{-/-}$ mice display early postnatal retinal and testicular degeneration [24] as well as leukodystrophy [25,26]; in humans, *CLCN2* loss-of-function mutations result in leukodystrophy[27] that may be associated with azoospermia[28]. These phenotypes have been ascribed to a role of ClC-2 in extracellular ion homeostasis [24,25].

Data retrieved from a transcriptome analysis including eleven human adrenals [29] showed high expression of *CLCN2* in human adrenal cortex (Supplementary Table 1). In mice, Western blots revealed similar expression of ClC-2 in whole adrenal gland as in brain (Fig. 2a), which expresses substantial, physiologically important amounts of ClC-2 [25]. Patch-clamp analysis of glomerulosa cells *in situ* revealed typical hyperpolarization-activated currents in WT, but not in *Clcn2*$^{-/-}$ mice (Fig. 2 b,c). Their magnitude was similar to those observed in Bergmann glia which prominently express ClC-2 [26]. The almost complete absence of Cl^- currents in *Clcn2*$^{-/-}$ cells demonstrates that under resting conditions ClC-2 mediates the bulk of glomerulosa cell Cl^- currents.

The *CLCN2* p.Gly24Asp mutation is located in a highly conserved 'inactivation domain' [2,3] of the channel. Deletions and point mutations in this region and an intracellular loop [2] (highlighted in Fig. 1c, d) lead to 'open' ClC-2 channels that have lost their sensitivity to voltage, cell swelling, or external pH [2,3]. Likewise, insertion of the p.Gly24Asp mutation drastically changed voltage-dependent gating of ClC-2 (Fig. 2d,e,h) and dramatically increased current amplitudes when expressed in *Xenopus* oocytes (Fig. 2d-g). When measured at -80 mV, the approximate resting potential of glomerulosa cells [30], current amplitudes from the mutant channel were much larger compared to WT (Fig. 2d-f). Linear, ohmic currents like those of the mutant channel might be due to unspecific electrical leaks; however, currents of both WT and mutant ClC-2 were markedly reduced when extracellular chloride was replaced by iodide (Fig. 2d-f), agreeing with the $Cl^->I^-$ selectivity of CLC channels in general [23] and ClC-2 in particular [1]. The activation of ClC-2 by acid extracellular pH can be almost abolished by mutations in the 'inactivation domain'[2]. Likewise, the ClC-2_{24Asp} mutant had largely reduced pH sensitivity (Fig. 2i-j, Supplementary Fig.1). In conclusion, the p.Gly24Asp mutation results in a strong gain of function, explaining the dominant disease phenotype of the mutation that is present at the heterozygote state. It also suggests a pathophysiological mechanism in which a strong increase in Cl^- currents may depolarize glomerulosa cells, thereby opening voltage-gated Ca^{2+} channels and activating transcriptional programs via an increase of cytosolic Ca^{2+}.

Expression of the mutant ClC-2_{24Asp} channel in adrenocortical H295R-S2 cells, and conversely, knock-down of ClC-2 by shRNA significantly affected aldosterone production and expression of steroidogenic enzymes. Despite similar expression of ClC-2 in H295R-S2 cells stably transfected with ClC-2_{24Asp} or ClC-2_{WT} (Fig. 3a and 3b), aldosterone synthase expression (Fig. 3a and 3c) and aldosterone production (Fig. 3d, e) were significantly increased in ClC-2_{24Asp} expressing cells. Stimulation with angiotensin II (AngII 10nM) or K^+

(12mM) increased aldosterone production in cells expressing WT ClC-2 (Fig. 3e). A further increase was observed in cells expressing ClC-2_{24Asp} after AngII stimulation, but not after K^+ stimulation (Fig. 3e). Nevertheless, also after stimulation, aldosterone production in cells expressing ClC-2_{24Asp} was significantly higher compared to cells expressing ClC-2_{WT} (Fig. 3e). Infection of H295R-S2 cells with ClC-2 shRNA reduced *CLCN2* expression by ~50% (Supplementary Fig. 2a) compared with a scrambled shRNA, and significantly reduced aldosterone production, both at baseline and after stimulation (Supplementary Fig. 2b), suggesting that even WT ClC-2 currents, although much smaller than currents from the Gly24Asp mutant, significantly increase the excitability of H295R-S2 adrenocortical cells. These changes were paralleled in both models by concomitant modifications of the expression of steroidogenic genes. A significant increase of mRNA expression of *CYP11B2* (encoding aldosterone synthase, Fig. 3f), *StAR* (encoding the Steroidogenic acute regulatory protein, Fig. 3g) and *CYP21A2* (encoding Steroid 21-hydroxylase, Fig. 3h) was observed in ClC-2_{24Asp} compared with ClC-2_{WT} overexpressing cells in basal conditions. AngII increased expression of *StAR* and *CYP11B2*, while K^+ stimulation increased mRNA expression of *CYP11B2*. Conversely, knock-down of ClC-2 led to a significant decrease in *CYP11B2* expression in all conditions (Supplementary Fig. 2c). These data further support the notion that a gain-of-function *CLCN2* mutation may depolarize the cell, activate the steroidogenic pathway, and increase aldosterone production. While knock-down of ClC-2 influences aldosterone production in H295R-S2 cells which have a resting potential of about – 65 mV (Fig. 4a, b), this may not be the case in native glomerulosa cells. Because their V_m is close to the K^+ equilibrium potential [30], they are unlikely to markedly hyperpolarize upon loss of ClC-2. No changes of blood pressure have been reported for mice or patients lacking ClC-2 [24,25,27], but this issue has not been investigated in detail.

We next explored the effect of the ClC-2 Gly24Asp mutation on the membrane potential and on calcium influx through voltage-gated calcium channels. These studies were performed with the perforated patch clamp technique which does not disturb the intracellular chloride concentration and is required to see the full effect of 'inactivation domain'[2,3] mutations[31,32]. In the stably transfected H295R-S2 cells used to investigate steroidogenesis (Fig. 3), there was a trend of V_m to be depolarized in ClC-2_{24Asp} transfected compared to ClC-2_{WT} transfected cells (mean values of roughly -52 and -67 mV, respectively) (Fig. 4a). However, because these cell lines are not clonal, the variability was large and the difference was not statistically significant.

We therefore resorted to transient transfection of H295R-S2 cells which allowed us to select ClC-2 expressing cells by fluorescence of co-transfected GFP (Fig. 4b-g). Although these cells express ClC-2 less efficiently than *Xenopus* oocytes (compare Fig. 4f and 2d) and HEK cells [31,32], ClC-2_{24Asp} expressing cells displayed robust chloride currents that lacked strong voltage-dependence (Fig. 4c-g). The observed increase in currents may reflect both an increase in currents per channel and in the number of channels; both must be considered when analyzing pathogenic effects of ion channel mutants. This increase in curents correlated with a strong depolarization from V_m= - 65 ± 4 (ClC-2_{WT}) to -46 ± 4 mV in ClC-2_{24Asp} transfected cells (Fig. 4b), indicating that chloride concentration in H295R-S2 cells is higher than predicted by the electrochemical equilibrium. This depolarization may open voltage-dependent calcium channels. Indeed, nifedipine (an L-type calcium channel blocker) and/or mibefradil (a T-type calcium channel blocker) strongly reduced aldosterone production in cells expressing the ClC-2_{24Asp} mutant (Fig. 4i). The involvement of L-type calcium channels appeared to be larger in ClC-2_{24Asp} expressing cells (Fig. 4h), possibly because of their depolarized plasma membrane potential which is required to open these channels [33]. However,

we cannot exclude that nifedipine acted partially through T-type calcium channels, which are also blocked by this compound at depolarized voltages[34].

To investigate whether the *CLCN2* p.Gly24Asp mutation could be involved in other forms of primary aldosteronism, we sequenced exon 2 of *CLCN2* in 100 patients with BAH. While *CLCN2* p.Gly24Asp was not identified among these subjects, we identified two rare *CLCN2* variants, c.197G>A (p.Arg66Gln, rs755883734) and c.143C>G (p.Pro48Arg, rs115661422) in two subjects (Supplementary Fig. 3). Minor allele frequencies of these variants are very low in the ExAC database (*CLCN2* p.Arg66Gln 0.00003; *CLCN2* p.Pro48Arg 0.0017). Both variants failed to significantly change ClC-2 currents in heterologous expression (Supplementary Fig. 4), in spite of a previously described[35] moderate reduction of ClC-$2_{Pro48Arg}$ current amplitudes. Nonetheless, it is noteworthy that the two patients were diagnosed with hypertension at young age, 29 and 19 ys respectively (Table 1) and in both cases during pregnancy. Finally, sequencing the *CLCN2* exons encoding the N-terminal domain (exon 1 and 2) and the loop between helices J and K (exon 10), corresponding to the ClC-2 'inactivation domains'[2,3], in 20 additional patients with hypertension before age 20 did not identify additional mutations. Among these patients, nine had a history of hypertension before the age of 15 years (one before age 10 ys), indicating that *CLCN2* mutations might underlie very young onset forms of primary aldosteronism.

In conclusion, we show that a gain-of-function mutation in the ClC-2 chloride channel underlies a genetic form of secondary arterial hypertension and identify ClC-2 as the foremost chloride conductor of resting glomerulosa cells. We suggest that increased Cl^- currents induced by the ClC-2 p.Gly24Asp mutation could depolarize the zona glomerulosa cell membrane, thereby opening voltage-gated calcium channels which trigger autonomous aldosterone production by increasing intracellular Ca^{2+} concentrations (Fig. 5b, red arrows). We hypothesize that the increased Cl^- currents may overcome the hyperpolarizing currents of

164 K^+ channels that normally determine the glomerulosa cell resting potential. The inhibition of
165 these potassium channels e.g. upon AngII stimulation, or the depolarizing currents mediated
166 by these channels upon increases in extracellular K^+, are the main mechanisms triggering
167 aldosterone production under physiological conditions (Fig. 5a, dashed black arrows).
168 Not only mutations in the amino-terminal ClC-2 'inactivation domain' [2,3], like the
169 Gly24Asp mutation found here, but also in the cytoplasmic linker between transmembrane
170 helices J and K may cause primary aldosteronism (Fig. 1d). Several point mutations in that
171 linker result in constitutively open ClC-2 channels [2]. We propose both regions as potential
172 hotspots for mutations causing primary aldosteronism. The discovery that a chloride channel
173 is involved in primary aldosteronism opens new and unexpected perspectives for the
174 pathogenesis and treatment of arterial hypertension.
175

Acknowledgements

This work was funded through institutional support from INSERM and by the Agence Nationale pour la Recherche (ANR-13-ISV1-0006-01), the Fondation pour la Recherche Médicale (DEQ20140329556), the Programme Hospitalier de Recherche Clinique (PHRC grant AOM 06179), and by institutional grants from INSERM. The laboratory of Dr. Maria-Christina Zennaro is also partner of the H2020 project ENSAT-HT grant n° 633983. Thomas J. Jentsch was supported by institutional funding from the Leibniz and Helmholtz Associations, a grant from the BMBF (E-RARE 01GM1403) and by the Prix Louis-Jeantet de Médecine.

Conflict of interest

The authors have nothing to disclose.

Author Contributions

MCZ, FFR, GD, IJO and TJJ designed experiments and wrote the manuscript. TMS, MCZ, TS and FFR performed and analyzed whole exome sequencing. MCZ, FFR, GD, REZ and SB performed and analyzed *in vitro* studies on H295R-S2 cells. IJO performed electrophysiological studies that were analyzed by IJO and TJJ. CG characterized adrenal glands from WT and *Clcn2*$^{-/-}$ mice and performed Western blots. VJ, XJ, LA, and HL were responsible for patients' recruitment, medical care and clinical data acquisition. All authors revised the manuscript draft.

References

1. Thiemann, A., Grunder, S., Pusch, M. & Jentsch, T.J. A chloride channel widely expressed in epithelial and non-epithelial cells. *Nature* **356**, 57-60 (1992).
2. Jordt, S.E. & Jentsch, T.J. Molecular dissection of gating in the ClC-2 chloride channel. *EMBO J.* **16**, 1582-92 (1997).
3. Grunder, S., Thiemann, A., Pusch, M. & Jentsch, T.J. Regions involved in the opening of CIC-2 chloride channel by voltage and cell volume. *Nature* **360**, 759-62 (1992).
4. Worldwide trends in blood pressure from 1975 to 2015: a pooled analysis of 1479 population-based measurement studies with 19.1 million participants. *Lancet* **389**, 37-55 (2017).
5. Hannemann, A. & Wallaschofski, H. Prevalence of primary aldosteronism in patient's cohorts and in population-based studies--a review of the current literature. *Horm. Metab. Res.* **44**, 157-62 (2012).
6. Calhoun, D.A. Hyperaldosteronism as a common cause of resistant hypertension. *Annu. Rev. Med.* **64**, 233-47 (2013).
7. Zennaro, M.C., Boulkroun, S. & Fernandes-Rosa, F. Genetic Causes of Functional Adrenocortical Adenomas. *Endocr. Rev.* **38**, 516-537 (2017).
8. Funder, J.W. *et al.* The Management of Primary Aldosteronism: Case Detection, Diagnosis, and Treatment: An Endocrine Society Clinical Practice Guideline. *J. Clin. Endocrinol. Metab.* **101**, 1889-916 (2016).
9. Savard, S., Amar, L., Plouin, P.F. & Steichen, O. Cardiovascular complications associated with primary aldosteronism: a controlled cross-sectional study. *Hypertension* **62**, 331-6 (2013).
10. Rossi, G.P. *et al.* A prospective study of the prevalence of primary aldosteronism in 1,125 hypertensive patients. *J. Am. Coll. Cardiol.* **48**, 2293-300 (2006).

11. Choi, M. *et al.* K+ channel mutations in adrenal aldosterone-producing adenomas and hereditary hypertension. *Science* **331**, 768-72 (2011).
12. Azizan, E.A. *et al.* Somatic mutations in ATP1A1 and CACNA1D underlie a common subtype of adrenal hypertension. *Nat. Genet.* **45**, 1055-60 (2013).
13. Scholl, U.I. *et al.* Somatic and germline CACNA1D calcium channel mutations in aldosterone-producing adenomas and primary aldosteronism. *Nat. Genet.* **45**, 1050-4 (2013).
14. Scholl, U.I. *et al.* Recurrent gain of function mutation in calcium channel CACNA1H causes early-onset hypertension with primary aldosteronism. *Elife* **4**, e06315 (2015).
15. Daniil, G. *et al.* CACNA1H Mutations Are Associated With Different Forms of Primary Aldosteronism. *EBioMedicine* **13**, 225-236 (2016).
16. Beuschlein, F. *et al.* Somatic mutations in ATP1A1 and ATP2B3 lead to aldosterone-producing adenomas and secondary hypertension. *Nat. Genet.* **45**, 440-4, 444e1-2 (2013).
17. Lifton, R.P. *et al.* A chimaeric 11beta-hydroxylase aldosterone synthase gene causes glucocorticoid-remediable aldosteronism and human hypertension. *Nature* **355**, 262-265 (1992).
18. Moss, S.J. & Smart, T.G. Constructing inhibitory synapses. *Nat. Rev. Neurosci.* **2**, 240-50 (2001).
19. Rinke, I., Artmann, J. & Stein, V. ClC-2 voltage-gated channels constitute part of the background conductance and assist chloride extrusion. *J. Neurosci.* **30**, 4776-86 (2010).
20. Koch, M.C. *et al.* The skeletal muscle chloride channel in dominant and recessive human myotonia. *Science* **257**, 797-800 (1992).

21. Guo, J.H. *et al.* Glucose-induced electrical activities and insulin secretion in pancreatic islet beta-cells are modulated by CFTR. *Nat. Commun.* **5**, 4420 (2014).
22. Chorvatova, A., Gendron, L., Bilodeau, L., Gallo-Payet, N. & Payet, M.D. A Ras-dependent chloride current activated by adrenocorticotropin in rat adrenal zona glomerulosa cells. *Endocrinology* **141**, 684-92 (2000).
23. Jentsch, T.J. Discovery of CLC transport proteins: cloning, structure, function and pathophysiology. *J. Physiol.* **593**, 4091-109 (2015).
24. Bosl, M.R. *et al.* Male germ cells and photoreceptors, both dependent on close cell-cell interactions, degenerate upon ClC-2 Cl(-) channel disruption. *EMBO J.* **20**, 1289-99 (2001).
25. Blanz, J. *et al.* Leukoencephalopathy upon disruption of the chloride channel ClC-2. *J. Neurosci.* **27**, 6581-9 (2007).
26. Hoegg-Beiler, M.B. *et al.* Disrupting MLC1 and GlialCAM and ClC-2 interactions in leukodystrophy entails glial chloride channel dysfunction. *Nat. Commun.* **5**, 3475 (2014).
27. Depienne, C. *et al.* Brain white matter oedema due to ClC-2 chloride channel deficiency: an observational analytical study. *Lancet Neurol.* **12**, 659-68 (2013).
28. Di Bella, D. *et al.* Subclinical leukodystrophy and infertility in a man with a novel homozygous CLCN2 mutation. *Neurology* **83**, 1217-8 (2014).
29. Boulkroun, S. *et al.* Prevalence, Clinical, and Molecular Correlates of KCNJ5 Mutations in Primary Aldosteronism. *Hypertension* **59**, 592-8 (2012).
30. Spat, A. & Hunyady, L. Control of aldosterone secretion: a model for convergence in cellular signaling pathways. *Physiol. Rev.* **84**, 489-539 (2004).

31. Varela, D., Niemeyer, M.I., Cid, L.P. & Sepulveda, F.V. Effect of an N-terminus deletion on voltage-dependent gating of the ClC-2 chloride channel. *J. Physiol.* **544**, 363-72 (2002).

32. Pusch, M., Jordt, S.E., Stein, V. & Jentsch, T.J. Chloride dependence of hyperpolarization-activated chloride channel gates. *J. Physiol.* **515 (Pt 2)**, 341-53 (1999).

33. Barrett, P.Q. *et al.* Role of voltage-gated calcium channels in the regulation of aldosterone production from zona glomerulosa cells of the adrenal cortex. *J. Physiol.* **594**, 5851-5860 (2016).

34. Perez-Reyes, E., Van Deusen, A.L. & Vitko, I. Molecular pharmacology of human Cav3.2 T-type Ca2+ channels: block by antihypertensives, antiarrhythmics, and their analogs. *J. Pharmacol. Exp. Ther.* **328**, 621-7 (2009).

35. Paul, J. *et al.* Alterations in the cytoplasmic domain of CLCN2 result in altered gating kinetics. *Cell. Physiol. Biochem.* **20**, 441-54 (2007).

36. Dutzler, R., Campbell, E.B., Cadene, M., Chait, B.T. & MacKinnon, R. X-ray structure of a ClC chloride channel at 3.0 A reveals the molecular basis of anion selectivity. *Nature* **415**, 287-94 (2002).

FIGURE LEGENDS

Figure 1. A *CLCN2* variant identified in a patient with early onset primary aldosteronism. (a) Pedigree of kindred K1011. The subject with PA is shown with a black symbol and non-affected subjects are shown with white symbols. (b) Sanger sequencing chromatograms showing the *CLCN2* wild-type sequence of the unaffected parents (K1011-3 and K1011-4) and brother (K1011-2) and the *CLCN2* variant c.71G>A (p.Gly24Asp) identified in the patient with early onset primary aldosteronism (K1011-1). (c) Alignment and conservation of residues encoded by *CLCN2* orthologs. The red box indicates the amino-terminal 'inactivation domain' of ClC-2. Several deletions and mutations in this region of rat ClC-2 led to constitutive open ClC-2 channels (uninterrupted line) or partially opened channels (dashed line) [3]. Residues that are conserved among more than 3 sequences are highlighted in yellow. (d) Position of the disease-causing Gly24Asp mutation in the ClC-2 protein (schematic transmembrane topology drawing modified from [36]). 'Inactivation domains' previously identified by structure-function analysis in the amino-terminus [3] and an intracellular loop [2] of ClC-2 are shown in red. Several point mutations and deletions in these domains open the ClC-2 channel [2,3] similar to the Gly24Asp substitution described here. CBS1 and CBS2, cystathionine-β-synthase domains which can affect gating of CLC channels [23].

Figure 2 ClC-2 expression in mouse adrenals and electrophysiological analyses of WT and mutant channels. (a) ClC-2 immunoblot of brain and adrenals from *Clcn2* $^{+/+}$ and *Clcn2* $^{-/-}$ mice. All lanes are from the same blot, which has been cut as indicated. Similar amounts of protein were loaded with actin serving as loading control. This blot is representative for three independent experiments. (b) Representative whole-cell chloride current traces of mouse zona glomerulosa cells from *Clcn2*$^{+/+}$ (top) and *Clcn2*$^{-/-}$ (bottom) adrenal slices using voltage steps as indicated above. (c) Mean ± SEM currents measured after 1.5 s from experiments in (b)

plotted as a function of clamp voltage. (d, e) Representative chloride current traces measured by two-electrode voltage-clamp from *Xenopus* oocytes injected with either human ClC-2_{WT} (d) or ClC-2_{24Asp} (e) cRNA, using the protocol shown in (d). For some measurements (below) extracellular chloride was replaced with iodide. (f) Mean ± SEM currents measured in (d,e) plotted as a function of voltage. Number of cells indicated in parenthesis. (g, h) Summary of Cl^- currents at -80 mV (I_{-80mV}) (g) and current ratios (I_{-120mV} / I_{+60mV}) as measure of rectification (h) (always measured at 2s) for panels (d-f). ****$p < 0.0001$, Mann-Whitney two-tailed test. (i, j) Effect of external pH on currents mediated by ClC-2_{WT} (i) or ClC-2_{24Asp} (j) in *Xenopus* oocytes. Currents were normalized to mean currents from respective construct measured after 2s at -120 mV and pH 7.4. Number of oocytes indicated in parenthesis, error bars indicate SEM.

Figure 3. Effect of ClC-2_{WT} and mutant ClC-2_{24Asp} channels on aldosterone production and expression of genes and proteins involved in aldosterone biosynthesis. (a) Western blots for ClC-2 and aldosterone synthase of H295R-S2 cells stably transfected with ClC-2_{WT} or mutant ClC-2_{24Asp}. These blots are representative of three independent experiments, with actin serving as loading control. (b) Quantification of ClC-2 protein expression in ClC-2_{WT} and ClC-2_{24Asp} H295R-S2 cells (T test p=0.10, F=3.19). (c) Quantification of aldosterone synthase expression in ClC-2_{WT} or ClC-2_{24Asp} H295R-S2 cells (T test p=0.0025, F=136). (d) Basal aldosterone production by H295R-S2 cells transfected with ClC-2_{WT} or mutant ClC-2_{24Asp} (T test, p=0.0008, F=142). (e) Basal and stimulated aldosterone production by H295R-S2 cells transfected with ClC-2_{WT} (open bars) or mutant ClC-2_{24Asp} (filled bars) (1way ANOVA p<0.0001, F=23.46). (f-h) Basal and stimulated mRNA expression of (f) *CYP11B2* (1way ANOVA p<0.001, F=18.39), (g) *STAR* (Kruskal-Wallys p=0.0033), and (h) *CYP21A2* (1way ANOVA p<0.0001, F23.27) in H295R-S2 cells transfected with ClC-2_{WT} (open bars) or

mutant ClC-2_{24Asp} (filled bars). Quantification of protein expression (using actin as loading control) and aldosterone production are represented as percentage of ClC-2_{WT} in basal conditions and results of mRNA expression are represented as fold induction of ClC-2_{WT} in basal conditions. Values of all experiments are represented as mean ± SEM of three independent experiments performed in experimental triplicates (n=9) for each condition. * $p<0.05$; ** $p<0.01$; *** $p<0.001$; i) $p<0.05$ stimulated vs basal condition, ii) $p<0.01$ stimulated vs basal condition; iii) $p<0.001$ stimulated vs basal condition.

Figure 4 Functional impact of the ClC-2_{24Asp} mutation. (a-g) Effect on membrane potential V_m and plasma membrane anion currents in H295R-S2 cells. (a) Resting membrane potential of ClC-2_{WT} and ClC-2_{24Asp} stably transfected H295R-S2 cells which were used to determine aldosterone secretion. Note strong mean depolarization (ClC-$2_{WT,}$ -67 ± 2 mV (n=8); ClC-$2_{24Asp,}$ -52 ± 6 mV (n=12)), which, however, was not significant (Two-tailed Mann-Whitney p = 0.14) owing to large variability of V_m of ClC-2_{24Asp} transfected cells that were not cloned. (b) Similarly determined values of V_m for non-transfected, and transiently transfected H295R-S2 cells (non-transfected, -65 ±4 mV (n=8); ClC-2_{WT}, -69 ± 7 mV (n=4); ClC-2_{24Asp}, -46 ± 4 mV (n=6); **, Two-tailed Mann-Whitney p = 0.0095)) (c,d) Corresponding plasma membrane currents measured after 1.5 s under conditions eliminating cation inward currents as function of voltage (c) or as plot of individual values at physiological V_m of glomerulosa cells (d) *, Two-tailed Mann-Whitney p = 0.019. (e-g) corresponding averaged current traces with 20 mV voltage steps between 0 and -120 mV. (h-i) Effect of calcium channel blockers on aldosterone production in H295R-S2 cells expressing (h) ClC-2_{WT} (Kruskall Wallis p=0.0005) and (i) ClC-2_{24Asp} (Kruskal Wallis, p=0.0032). Values represent mean ± SEM of two independent experiments performed in experimental triplicates (n=6) for each condition. * $p<0.05$; ** $p<0.01$.

Figure 5. Proposed model for autonomous aldosterone secretion in adrenal zona glomerulosa cells with the ClC-2_{24Asp} mutation. (a) In unstimulated conditions, the ZG cell membrane potential closely follows the potassium resting potential at approximately -80 mV. Increasing extracellular K^+ concentration, or inhibition of K^+ channels by AngII through its receptor (AT1R), leads to cell membrane depolarization, opening of voltage-gated Ca^{2+} channels, and increased intracellular calcium concentrations, the major trigger for aldosterone biosynthesis. Binding of AngII to AT1R also leads to Gαq-mediated signaling and IP3-mediated release of Ca^{2+} from the endoplasmic reticulum. (b) The ClC-2 p.Gly24Asn mutation abolishes the voltage-dependent gating of ClC-2. The resulting pronounced increase of Cl^- currents at resting potentials is proposed to result in cell depolarization, opening of voltage gated Ca^{2+} channel, stimulation of Ca^{2+} signaling, and finally increased expression of steroidogenic genes and aldosterone production.

Table 1. Clinical and biological characteristics of patients carriers of *CLCN2* variants.

	K1011-1	K963-1	K1044-1
Sex	F	F	F
Age at HTN dg (ys)	9	19	29
Age at primary aldosteronism dg (ys)	9	27	48
SBP at primary aldosteronism dg (mmHg)	172	139	173
DBP at primary aldosteronism dg (mmHg)	100	90	114
Lowest plasma K^+ (mmol/L)	1.8	2.9	2.5
Urinary aldosterone (nmol/24h)	ND	60	ND
Plasma aldosterone (pmol/L)[a]	2406	927	1061
Plasma renin (mU/L)[a]	0.9	1.9	<1
ARR (pmol/mU)[b]	481.2	185.4	212.2
Adrenal abnormalities on imaging	No	No	No
Lateralization at AVS	ND	No	No

dg, diagnosis; m, months; y, years ; HTN, hypertension; SBP, systolic blood pressure; DBP, diastolic blood pressure; K, potassium; ARR, aldosterone to renin ratio; Hormonal data are at diagnosis of primary aldosteronism. ND, not determined. For comparison within this table, plasma aldosterone levels for patient K1011-1 have been converted to pmol/L and plasma renin activity to plasma renin concentration. [b]for ARR calculation, renin values <5 have been transformed to 5. Conversion factor used for plasma aldosterone: 1 ng/l = 2.77 pmol/L; conversion factor used for plasma renin: 1 ng/ml/h = 8.2 mU/L.

Online Methods

Patients

Patients with primary aldosteronism were recruited within the COMETE (COrtico- et MEdullo-surrénale, les Tumeurs Endocrines) network (COMETE-HEGP protocol, authorization CPP 2012-A00508-35) or in the context of genetic screening for familial hyperaldosteronism at the Genetics department of the HEGP. Methods for screening and subtype identification of primary aldosteronism were performed according to the Endocrine Society guidelines[8]. In patients diagnosed with primary aldosteronism, a thin slice CT scan or MRI of the adrenal and/or an adrenal venous sampling (AVS) were performed to differentiate between unilateral and bilateral aldosterone hypersecretion. All patients gave written informed consent for genetic and clinical investigation. Procedures were in accordance with institutional guidelines.

DNA isolation

DNA from peripheral blood leukocytes was extracted using QIAamp DNA midi kit (Qiagen, Courtaboeuf Cedex, France) or salt-extraction.

Whole exome sequencing and variant detection

Exomes were enriched in solution and indexed with SureSelect XT Human All Exon 50 Mb kits (Agilent). Sequencing was performed as 100 bp paired-end runs on HiSeq2000 systems (Illumina). Pools of 12 indexed libraries were sequenced on four lanes. Image analysis and base calling was performed using Illumina Real Time Analysis. CASAVA 1·8 was used for demultiplexing. BWA (v 0.5.9) with standard parameters was used for read alignment against the human genome assembly hg19 (GRCh37). We performed single-nucleotide variant and small insertion and deletion (indel) calling specifically for the regions targeted by the exome

enrichment kit, using SAMtools (v 0.1.18). Subsequently the variant quality was determined using the SAMtools varFilter script. We used default parameters, with the exception of the maximum read depth (-D) and the minimum P-value for base quality bias (-2), which we set to 9999 and 1e-400, respectively. Additionally, we applied a custom script to mark all variants with adjacent bases of low median base quality. All variants were then annotated using custom Perl scripts. Annotation included information about known transcripts (UCSC Known Genes and RefSeq genes), known variants (dbSNP v 135), type of mutation, and - if applicable – amino acid change in the corresponding protein. The annotated variants were then inserted into our in-house database. To reduce false positives we filtered out variants that were already present in our database, had variant quality less than 40, or failed one of the filters from the filter scripts. We then manually investigated the raw read data of the remaining variants using the Integrative Genomics Viewer (IGV).

Sanger sequencing

CLCN2 DNA was amplified using the intron-spanning primers described in supplementary table S2. PCR were performed on 100 ng of DNA in a final volume of 25 µl containing 0.75 mM $MgCl_2$, 400 nM of each primer, 200 µM deoxynucleotide triphosphate, and 1.25 U Taq DNA Polymerase (Sigma). Cycling conditions for *CLCN2* were as previously described [37] with an annealing temperature of 60°C. Direct sequencing of PCR products was performed using the ABI Prism Big Dye Terminator® v3.1 Cycle Sequencing Kit (Applied Biosystems, Foster City, CA) on an ABI Prism 3700 DNA Analyzer (Applied Biosystems).

Site directed mutagenesis

The ClC-2_{24Asp} construct was generated by site-directed mutagenesis using the QuikChange II XL site-directed mutagenesis kit (Agilent). The mutation was introduced into the human ClC-

2 cDNA fragment inserted into the pFROG expression vector [38] and their presence confirmed by Sanger sequencing.

Western blot

The membrane fractions of tissue homogenate from brain and adrenal gland of adult *Clcn2* $^{+/+}$ and *Clcn2* $^{-/-}$ mice were isolated and lysed in 50mM Tris pH 6.8, 140mM NaCl, 0.5mM EDTA and 2% SDS with protease inhibitors (4 mM Pefabloc and Complete® EDTA-free protease inhibitor cocktail, Roche). Equal amounts of protein were separated by SDS–PAGE (10 % polyacrylamide) and blotted onto nitrocellulose. Rabbit polyclonal antibodies against a modified carboxy-terminal ClC-2 peptide have been described previously [26]. Blots were reprobed with mouse anti-β-actin (Clone AC-74, Sigma A2228, 1:1000) as a loading control. H295R-S2 cells were lysed using RIPA buffer (Bio Basic Canada Inc.) with protease and phosphatase inhibitors mini tablets, EDTA free (Thermo Scientific). Proteins were solubilized for 30 min at 4°C, under end-over-end rotation, and then centrifuged at 13000 rpm for 15 min at 4°C. Equal amounts of proteins were submitted to 10% SDS-PAGE and transferred onto nitrocellulose membrane. Membranes were blotted with rabbit anti-ClC-2 antibody (1:500), mouse anti-aldosterone synthase antibody (1:500, clone CYP11B2-41-13, kindly provided by Dr C Gomez Sanchez[39]) and mouse anti-β-actin (A2228, 1:10000, Sigma).

Electrophysiological recordings

Patch clamp analysis were performed in adrenal sections from wild type and *Clcn2*$^{-/-}$ mice [24], similarly to previously described [40]. Bicarbonate based buffers were used which were continuously bubbled with 95% O_2 and 5% CO_2. Briefly, adrenal glands were removed and placed into cold low-Ca^{2+} solution composed of (in mM): 140 NaCl, 2 KCl, 26 $NaHCO_3$, 10

463 glucose, 5 $MgCl_2$, 0.1 $CaCl_2$, pH 7.4. The adrenals, after removal of surrounding fat tissue,
464 were embedded in 3% low-melting agarose, sectioned at 70 µm (Leica VT1200S), and
465 incubated at room temperature in solution containing: 140 NaCl, 2 KCl, 26 $NaHCO_3$, 10
466 glucose, 2 $MgCl_2$, 2 $CaCl_2$, and adjusted to pH 7.4. After at least 1 hour, slices were then
467 transferred to a recording chamber and imaged with a 60x objective and DIC optics (Olympus
468 BX51WI). Cells of the zona glomerulosa were identified by their rosette organization.
469 Electrical signals were acquired at room temperature using a microelectrode amplifier
470 (Multiclamp 700B) and software (Clampex 10.3, Molecular Devices, USA). As expected,
471 cells when patched with a K^+-based solution displayed spontaneous spiking which could be
472 stimulated with angiotensin II. For measuring chloride currents, patch pipettes were filled
473 with solution containing: 117.5 $CsMeSO_3$, 17.5 CsCl, 4 NaCl, 10 Hepes, 1 EGTA, 1 $MgCl_2$,
474 adjusted to pH 7.3 while the bath solution contained: 117 NMDG-Cl, 23 NMDG-HCO_3, 5
475 CsCl, 1.3 $MgCl_2$, 9 glucose, 2 $CaCl_2$, adjusted to pH 7.3. Voltage steps from +40 to −120 mV
476 from a holding potential of −10 mV were used, with a final 1 s step at +40 mV. Signals were
477 digitized at 10 kHz, filtered at 2 kHz and stored off-line for analysis with Clampfit software
478 10.4.
479 For two electrode voltage clamp in *Xenopus laevis* oocytes, human wildtype and Gly24Asp
480 ClC-2 cRNAs were prepared from pFROG vectors (Ambion mMESSAGE mMACHINE T7
481 kit) and injected into *X. laevis* oocytes, 13.8 ng and 9.2 ng per cell, respectively. Following
482 two days of expression at 17°C, two electrode voltage clamp was performed at room
483 temperature using a TurboTEC amplifier (npi electronic GmbH, Tamm, Germany) and
484 pClamp Software (Molecular Devices) to elicit ClC-2 currents (2s steps from +60mV to -
485 120mV with a final 1s step at +40mV) in ND109 solution containing (in mM): 109 NaCl, 2
486 KCl, 1 $MgCl_2$, 1.8 $CaCl_2$, 2 HEPES and adjusted to pH 7.4. To test for the typical $Cl^->I^-$
487 selectivity of CLC channels, currents were sequentially measured in solutions containing 109

mM Cl^- or 109 mM I^-. To determine the pH sensitivity of currents, ND109 was buffered with 5 mM MES for pH 6.5 and with 5 mM Tris for pH 8.5. Off-line analysis was performed with Clampfit software 10.4. Statistical significance was assessed using the Mann–Whitney test (Prism, GraphPad Software, USA).

For patch clamp of transiently transfected H295R-S2 cells, cells were seeded at 30% confluency onto poly-L-lysine (Sigma) coated glass coverslips. Once adhered they were transfected (X-fect) with bicistronic plasmids encoding emGFP (for identification of transfected cells) and, after an an IRES sequence, $ClC\text{-}2_{WT}$ or $ClC\text{-}2_{G24D}$. Cells were measured 12-24 hours later. Both transiently and stably transfected cells were measured using a Multiclamp 700B (Axon Instruments) amplifier Gramicidin-perforated patch clamp was performed to retain the intracellular chloride concentration. The tips of patch pipettes were first filled with gramicidin-free internal pipette solution (in mM): 100 $KMeSO_3$, 30 KCl, 4 NaCl, 10 Hepes, 1 $MgCl_2$, 1 EGTA, 3 MgATP (pH 7.3, 280 mOsm/L) and then back-filled with the same solution containing 25µg/mL gramicidin. GFP expressing cells were selected for analysis. Approximately 20 minutes following tight giga-seal formation, stable membrane potential measurements (I=0 configuration) could be acquired with access resistances of <100 MΩ in bath solution containing 140 NaCl, 5 KCl, 10 Hepes, 1.8 $MgCl_2$, 1.8 $CaCl_2$ (pH 7.4, 300 mOsm/L). When adequate access resistance was attained (<35 MΩ), a Na^+- and K^+-free bath solution containing 140 CsCl, 10 Hepes, 1.8 $MgCl_2$, 1.8 $CaCl_2$, 20 sucrose (pH 7.3, 300 mOsm/L) was perfused to measure anion membrane currents in the voltage clamp configuration (1s steps from +60 mV to -120 mV from a holding clamp of -10 mV). Measurements were performed at room temperature (22-24°C). Data are presented as mean ± SEM.

Functional studies in H295R-S2 cells

513 The human adrenocortical carcinoma cell line H295R strain 2 (H295R-S2), kindly
514 provided by W. E. Rainey [41] was cultured in DMEM/Eagle's F12 medium (GIBCO, Life
515 technologies, Carlsbad, CA) supplemented with 2% Ultroser G (PALL life sciences, France),
516 1% insulin/transferrin/selenium Premix (GIBCO, Life technologies, Carlsbad, CA), 10mM
517 HEPES (GIBCO, Life technologies, Carlsbad, CA), 1% penicillin, and streptomycin (GIBCO,
518 Life technologies, Carlsbad, CA) and maintained in a 37°C humidified atmosphere (5%
519 CO2).
520 For overexpression experiments, H295R-S2 cells were seeded into tissue culture dishes 100 in
521 groups of 5.000·000 cells per dish, and maintained in the conditions described. After 24h,
522 cells were resuspended in 100 µl Nucleofector R solution (AMAXA kit, Lonza) and
523 transfected with 3 µg of the ClC-2_{WT} or ClC-2_{24Asp} pFROG construct or a GFP construct,
524 using the electroporation program P-20. To select only stably transfected cells, 48h post
525 transfection cells were changed to medium containing 500 µg/mL G418-Genetycin (Gibco)
526 and used after all GFP transfected cells were dead. G418 selection was kept during all
527 functional studies. For aldosterone measurements and RNA extraction, cells were serum
528 deprived in DMEM/F12 containing 0.1% Ultroser G for 24h and then incubated for another
529 24h with fresh medium containing 0.1% Ultroser G with no secretagogue or vehicle (basal),
530 or secretagogues AngII (10nM) or K^+ (12mM), or calcium channel bloquers Nifedipine (L-
531 Type calcium channel blocker, 10µM, Sigma) or Mibefradil (T-type calcium channel
532 blocker, 10µM, Sigma). At the end of the incubation time, supernatant and cells from each
533 well were harvested for aldosterone measurement and RNA extraction. Three experiments
534 using aldosterone secretagogues (n=9) and two experiments using calcium channel blockers
535 (n=6) were independently conducted in triplicate.
536 Human ClC2-targeting (TRCN0000427876) and non-mammalian control (SHC002V)
537 MISSION shRNA lentiviral transduction particles were obtained from Sigma-Aldrich. The

shRNA sequences were inserted into TRC2 pLKO-puro plasmid backbone. For the lentiviral infections, manufacturer's protocol was followed with slight modifications. 1 x 10^4 H295R-S2 cells were seeded in a 96-well plate. After 24 hours, medium was changed and supplemented with 2 µg/ml polybrene (Sigma). Lentiviral particles were then added at a multiplicity of infection of 10 and medium changed after overnight incubation. For selection, 2 µg/ml puromycin (Gibco) was added to the medium. After two passages cells were characterized in terms of mRNA expression and aldosterone production after incubation with or without secretagogue as mentioned above.

RNA extraction and RT-qPCR

Total RNA was extracted in Trizol reagent (Ambion Life technologies, Carlsbad CA) according to the manufacturer's recommendations. After deoxyribonuclease I treatment (Life Technologies, Carlsbad, CA), 500 ng of total RNA were retrotranscribed (iScript reverse transcriptase, Biorad, Hercules, CA). Primers used for qPCR are described in supplementary table 3. The quantitative PCR was performed using SYBRgreen (Sso advanced universal SyBr Green supermix, Biorad, Hercules, CA) on a C1000 touch thermal cycler of Biorad (CFX96 Real Time System), according to the manufacturer's instructions. Controls without template were included to verify that fluorescence was not overestimated from primer dimer formation or PCR contaminations. RT-qPCR products were analyzed in a post amplification fusion curve to ensure that a single amplicon was obtained. Normalization for RNA quantity, and reverse transcriptase efficiency was performed against three reference genes (geometric mean of the expression of Ribosomal *18S* RNA, *HPRT*, and *GAPDH*), in accordance with the MIQE guidelines [42]. Quantification was performed using the standard curve method. Standard curves were generated using serial dilutions from a cDNA pool of all samples of each experiment, yielding a correlation coefficient of at least 0.98 in all experiments.

563

564 ***Aldosterone and protein assays***

565 Aldosterone levels were measured in cell culture supernatants by ELISA. Aldosterone
566 antibody and aldosterone-3-CMO-biotin were kindly provided by Dr Gomez-Sanchez [43].
567 Aldosterone concentrations were normalized to cell protein concentrations (determined using
568 Bradford protein assay).

569

570 ***Statistical analyses***

571 Quantitative variables are reported as means ± standard error of the mean (SEM) when
572 Gaussian distribution or medians and interquartile range when no Gaussian distribution.
573 Pairwise comparisons were done with unpaired t-test or Mann-Whitney test respectively;
574 multiple comparisons were done with the ANOVA test followed by a test for pairwise
575 comparison of subgroups according to Bonferroni when Gaussian distribution, or Kruskal-
576 Wallis followed by Dunn's test when no Gaussian distribution. Comparisons between two
577 groups were performed with two-tailed T test or two-tailed Mann-Whitney test. A p value <
578 0.05 was considered significant. For functional experiments, all results were expressed as
579 mean ± SEM of three separate experiments performed in triplicate for ClC-2 overexpression
580 studies with secretagogues, two separate experiments performed in triplicate for ClC-2
581 expression studies with calcium channel blockers, and two to four separate experiments
582 performed in triplicate for ClC-2 knockdown studies. Analyses were performed using Prism5
583 (GraphPad software Inc, San Diego, CA).

584

585 **Data availability.**

The data that support the findings of this study are available from the authors on reasonable request, see author contributions for specific data sets. Disease-causing variants have been submitted to ClinVar. Exome data are available on request within a scientific cooperation.

Online Methods References

37. Hubert, E.L. *et al.* Mineralocorticoid receptor mutations and a severe recessive pseudohypoaldosteronism type 1. *J. Am. Soc. Nephrol.* **22**, 1997-2003 (2011).

38. Gunther, W., Luchow, A., Cluzeaud, F., Vandewalle, A. & Jentsch, T.J. ClC-5, the chloride channel mutated in Dent's disease, colocalizes with the proton pump in endocytotically active kidney cells. *Proc. Natl. Acad. Sci. U S A* **95**, 8075-80 (1998).

39. Gomez-Sanchez, C.E. *et al.* Development of monoclonal antibodies against human CYP11B1 and CYP11B2. *Mol. Cell. Endocrinol.* **383**, 111-7 (2014).

40. Hu, C., Rusin, C.G., Tan, Z., Guagliardo, N.A. & Barrett, P.Q. Zona glomerulosa cells of the mouse adrenal cortex are intrinsic electrical oscillators. *J. Clin. Invest.* **122**, 2046-53 (2012).

41. Wang, T. *et al.* Comparison of aldosterone production among human adrenocortical cell lines. *Horm. Metab. Res.* **44**, 245-50 (2012).

42. Bustin, S.A. *et al.* The MIQE guidelines: minimum information for publication of quantitative real-time PCR experiments. *Clin. Chem.* **55**, 611-22 (2009).

43. Gomez-Sanchez, C.E. *et al.* The production of monoclonal antibodies against aldosterone. *Steroids* **49**, 581-7 (1987).

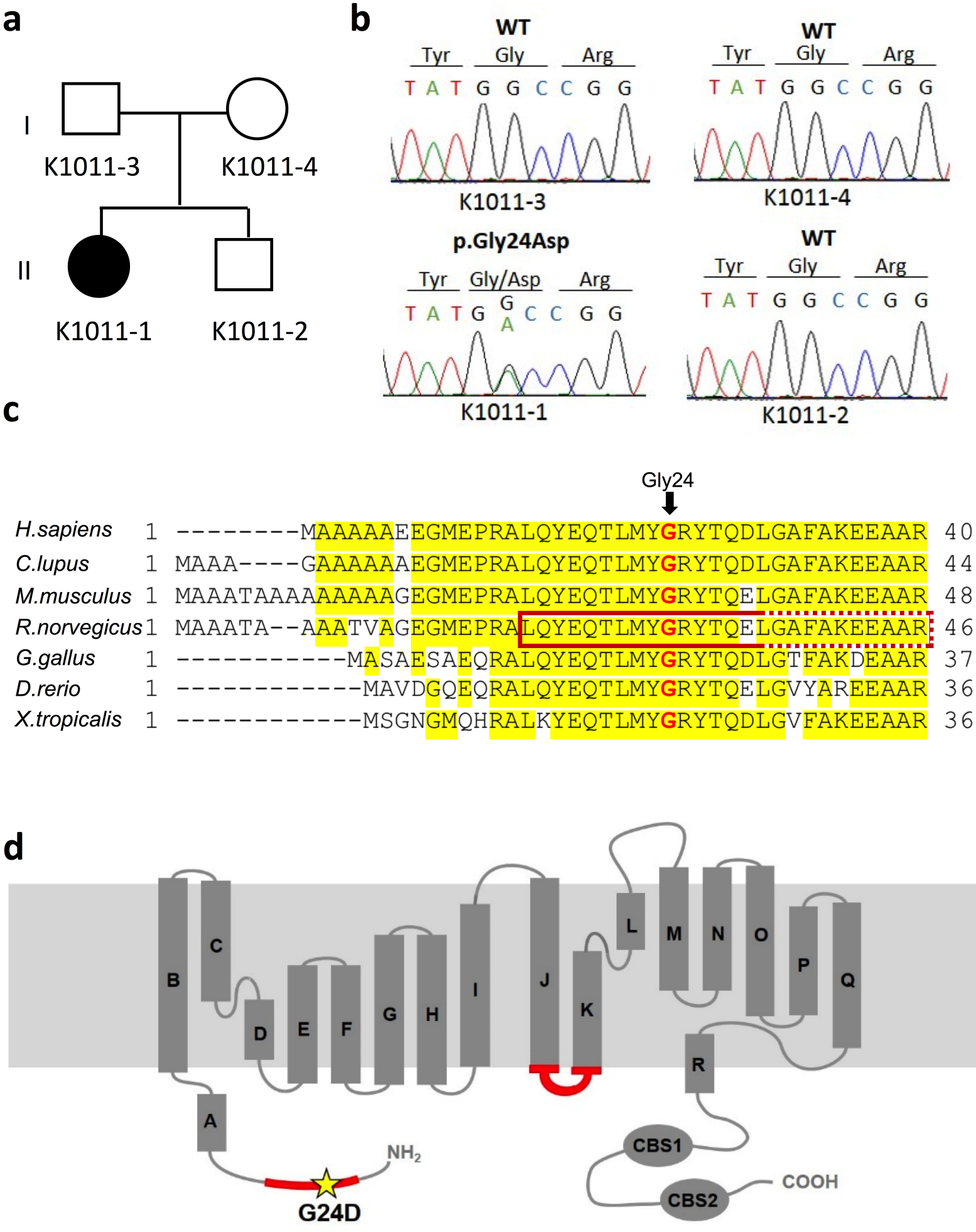
a
I
K1011-3
K1011-4
II
K1011-1
K1011-2
b
WT
Tyr Gly Arg
T A T G G C C G G
K1011-3
WT
Tyr Gly Arg
T A T G G C C G G
K1011-4
p.Gly24Asp
Tyr Gly/Asp Arg
T A T G G C C G G
A
K1011-1
WT
Tyr Gly Arg
T A T G G C C G G
K1011-2
c
Gly24
H.sapiens 1 --------MAAAAAEEGMEPRALQYEQTLMYGRYTQDLGAFAKEEAAR 40
C.lupus 1 MAAA----GAAAAAAEGMEPRALQYEQTLMYGRYTQDLGAFAKEEAAR 44
M.musculus 1 MAAATAAAAAAAAAGEGMEPRALQYEQTLMYGRYTQELGAFAKEEAAR 48
R.norvegicus 1 MAAATA--AAATVAGEGMEPRALQYEQTLMYGRYTQELGAFAKEEAAR 46
G.gallus 1 ----------MASAESAEQRALQYEQTLMYGRYTQDLGTFAKDEAAR 37
D.rerio 1 ----------MAVDGQEQRALQYEQTLMYGRYTQELGVYAREEAAR 36
X.tropicalis 1 ----------MSGNGMQHRALKYEQTLMYGRYTQDLGVFAKEEAAR 36
d
A
B
C
D
E
F
G
H
I
J
K
L
M
N
O
P
Q
R
NH2
G24D
CBS1
CBS2
COOH

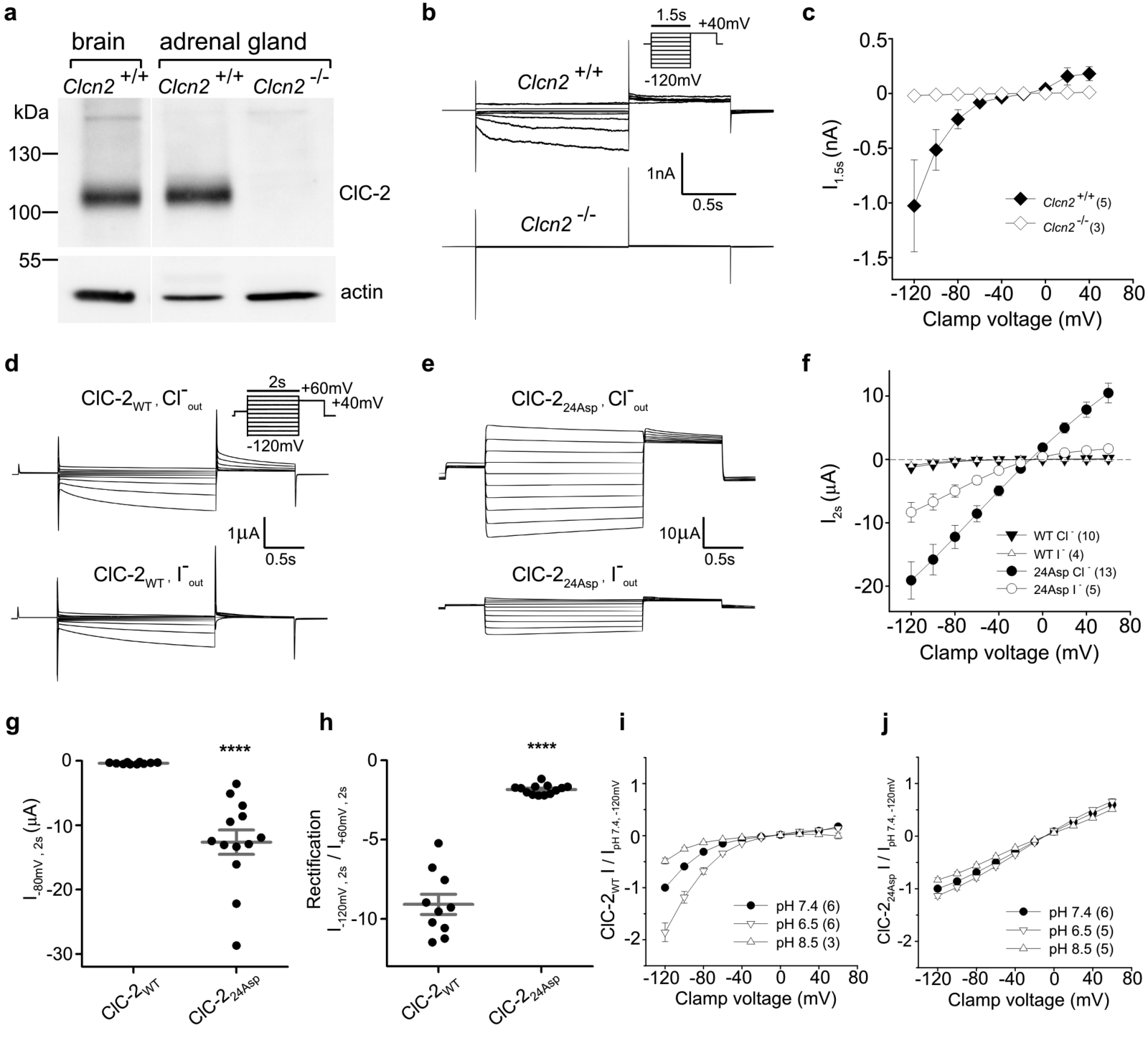
a
brain
adrenal gland
Clcn2 +/+
Clcn2 +/+
Clcn2 -/-
kDa
130
100
55
ClC-2
actin
b
1.5s
+40mV
-120mV
Clcn2 +/+
1nA
0.5s
Clcn2 -/-
c
I1.5s (nA)
Clcn2 +/+ (5)
Clcn2 -/- (3)
Clamp voltage (mV)
d
ClC-2WT , Cl-out
2s
+60mV
+40mV
-120mV
1µA
0.5s
ClC-2WT , I-out
e
ClC-2 24Asp , Cl-out
10µA
0.5s
ClC-2 24Asp , I-out
f
I2s (µA)
WT Cl- (10)
WT I- (4)
24Asp Cl- (13)
24Asp I- (5)
Clamp voltage (mV)
g
I-80mV , 2s (µA)
****
ClC-2WT
ClC-2 24Asp
h
Rectification
I-120mV , 2s / I+60mV , 2s
****
ClC-2WT
ClC-2 24Asp
i
ClC-2WT I / IpH 7.4, -120mV
pH 7.4 (6)
pH 6.5 (6)
pH 8.5 (3)
Clamp voltage (mV)
j
ClC-2 24Asp I / IpH 7.4, -120mV
pH 7.4 (6)
pH 6.5 (5)
pH 8.5 (5)
Clamp voltage (mV)

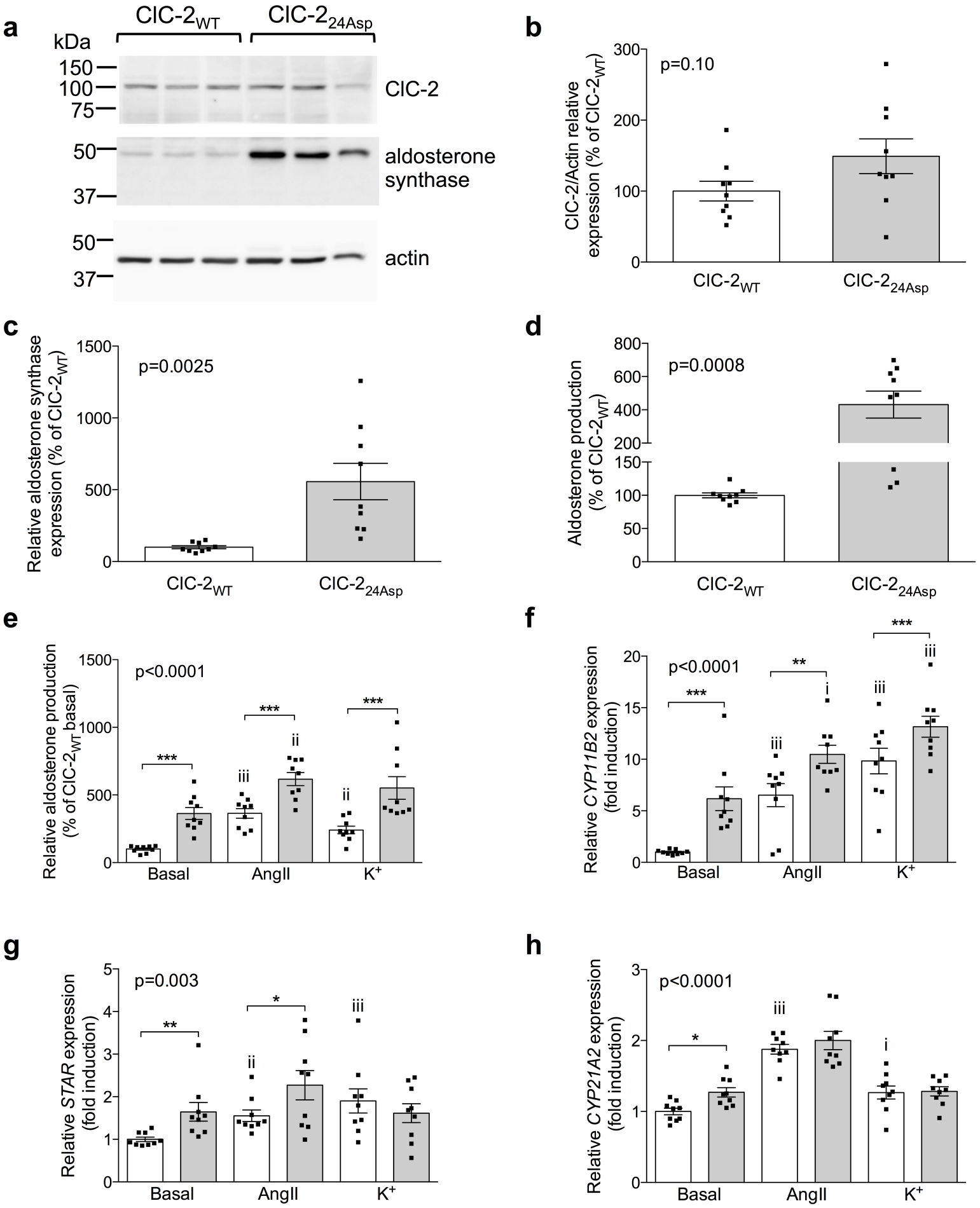
a
ClC-2WT
ClC-224Asp
kDa
150
100
75
ClC-2
50
37
aldosterone synthase
50
37
actin
b
p=0.10
ClC-2/Actin relative expression (% of ClC-2WT)
300
200
100
0
ClC-2WT
ClC-224Asp
c
p=0.0025
Relative aldosterone synthase expression (% of ClC-2WT)
1500
1000
500
0
ClC-2WT
ClC-224Asp
d
p=0.0008
Aldosterone production (% of ClC-2WT)
800
600
400
200
150
100
50
0
ClC-2WT
ClC-224Asp
e
p<0.0001
Relative aldosterone production (% of ClC-2WT basal)
1500
1000
500
0
***
***
***
iii
ii
ii
Basal
AngII
K+
f
p<0.0001
Relative CYP11B2 expression (fold induction)
20
15
10
5
0
***
**
***
iii
i
iii
Basal
AngII
K+
g
p=0.003
Relative STAR expression (fold induction)
5
4
3
2
1
0
**
*
ii
iii
Basal
AngII
K+
h
p<0.0001
Relative CYP21A2 expression (fold induction)
3
2
1
0
*
iii
i
Basal
AngII
K+

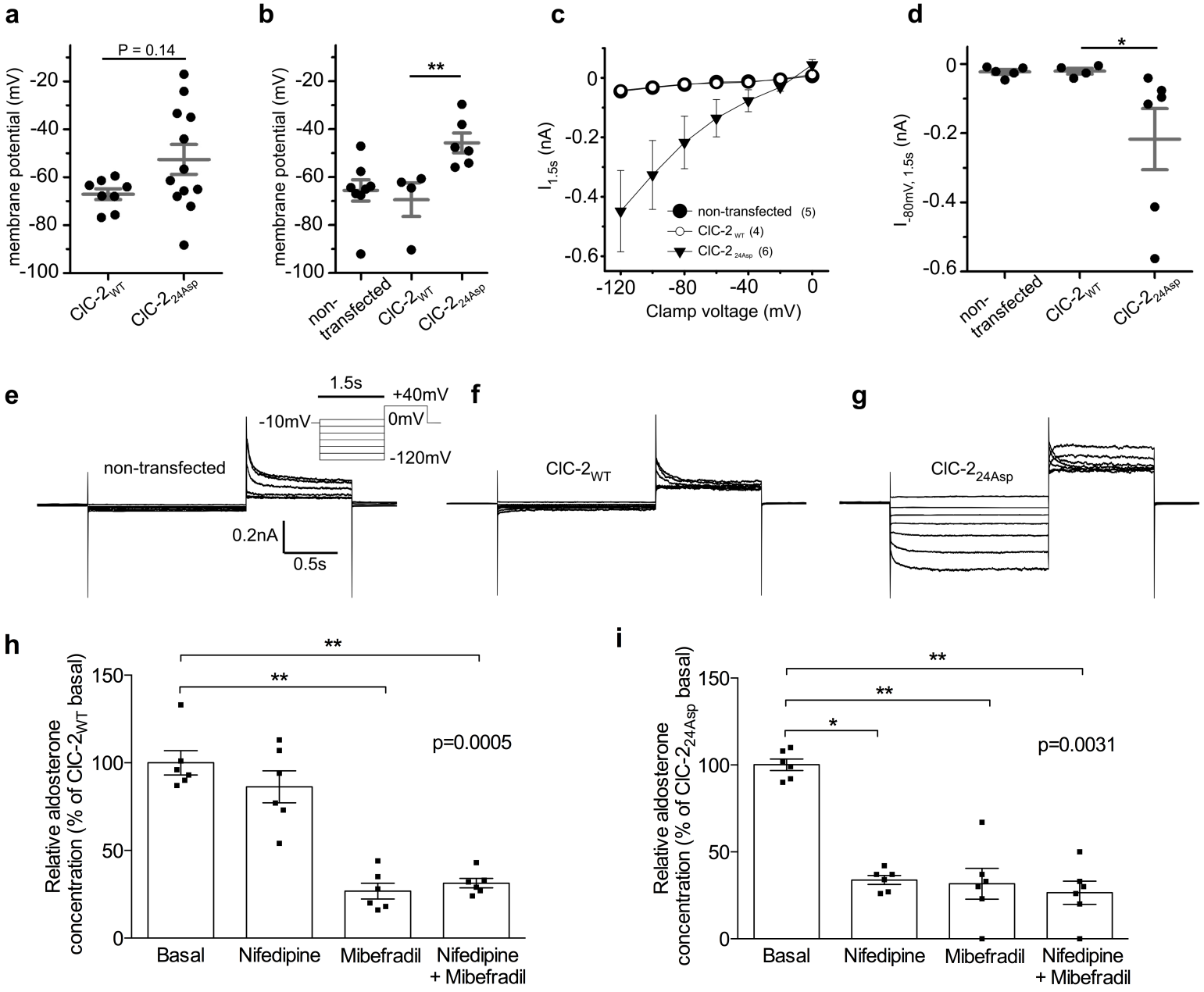
a
P = 0.14
membrane potential (mV)
-20
-40
-60
-80
-100
ClC-2WT
ClC-2 24Asp
b
**
membrane potential (mV)
non-transfected
ClC-2WT
ClC-2 24Asp
c
I1.5s (nA)
0
-0.2
-0.4
-0.6
non-transfected (5)
ClC-2 WT (4)
ClC-2 24Asp (6)
-120
-80
-40
0
Clamp voltage (mV)
d
*
I-80mV, 1.5s (nA)
0
-0.2
-0.4
-0.6
non-transfected
ClC-2WT
ClC-2 24Asp
e
1.5s
+40mV
-10mV
0mV
-120mV
non-transfected
0.2nA
0.5s
f
ClC-2WT
g
ClC-2 24Asp
h
**
**
Relative aldosterone concentration (% of ClC-2WT basal)
150
100
50
0
p=0.0005
Basal
Nifedipine
Mibefradil
Nifedipine + Mibefradil
i
**
**
*
Relative aldosterone concentration (% of ClC-2 24Asp basal)
150
100
50
0
p=0.0031
Basal
Nifedipine
Mibefradil
Nifedipine + Mibefradil

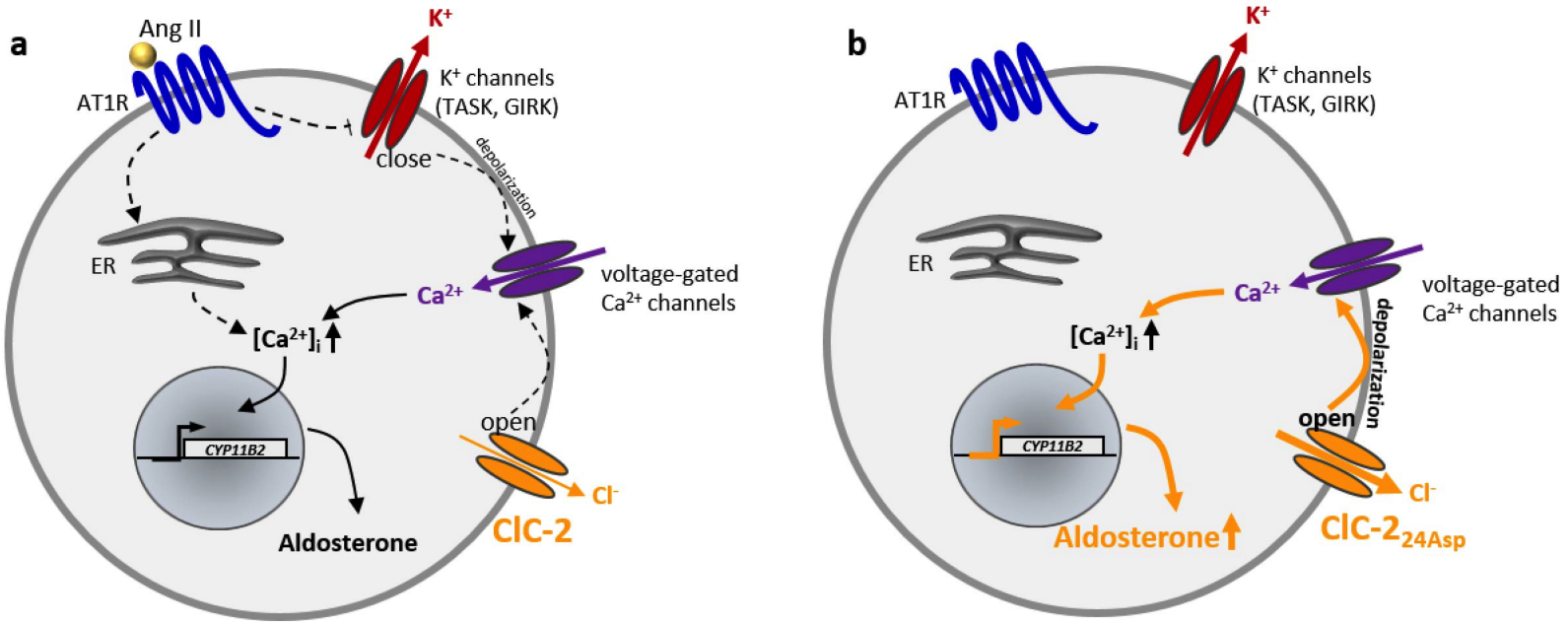
a
Ang II
AT1R
K+
K+ channels
(TASK, GIRK)
close
depolarization
ER
Ca2+
voltage-gated
Ca2+ channels
[Ca2+]i
CYP11B2
open
Cl-
Aldosterone
ClC-2
b
K+
K+ channels
(TASK, GIRK)
AT1R
ER
Ca2+
voltage-gated
Ca2+ channels
[Ca2+]i
depolarization
CYP11B2
open
Cl-
Aldosterone
ClC-2 24Asp